Magnetic Resonance Elastography: A Method for the Noninvasive and Spatially Resolved Observation of Phase Transitions in Gels

Ingolf Sack, Gerd Buntkowsky,† Johannes Bernarding, and Juergen Braun*

Department of Medical Informatics
University Hospital Benjamin Franklin
Hindenburgdamm 30, 12200 Berlin, Germany
Department of Organic Chemistry
Free University Berlin, Takustrasse 9
14195 Berlin, Germany

Received May 4, 2001

Dynamic magnetic resonance elastography (MRE) is a new imaging technique[1] recently developed for the noninvasive determination of biomechanical properties of biological tissue.[2] Compared to traditional medical palpation techniques, MRE is characterized by a high spatial resolution and a high sensitivity to the varying stiffness between healthy and pathologic tissues even in nonaccessible body regions.[3] Moreover, MRE also provides new information for other research fields. We report the spatially and temporally resolved observation of the sol/gel phase transition in a thermo-reversible gel. Observed wave patterns were reproduced using a model calculation based on temperature-dependent biomechanical properties of the sample.

Dynamic MRE is based on the visualization of propagating shear waves in harmonically excited samples. The shear waves are usually generated mechanically with excitation frequencies between 50 and 600 Hz.[1] Minimum amplitudes for particle displacement are in the order of 0.1 μm. This enables the transmission of shear waves with low damping into the sample. The wave patterns, which depend on the local biomechanical properties of the sample, are visualized by using motion-sensitive MRI techniques.[1] Maps of local shear stiffness or shear moduli (elastograms) can be reconstructed from the wave images.[4]

The gel phantom was prepared by dissolving 22.5 g of agar (1.5%) in 1.5 L of water heated to 90 °C. The fluid gel was examined in a double-walled container open at the top. The cooling of the sample (total cooling time 5 h), monitored with a thermometer between 60 and 25 °C, showed an exponential time dependence. Shear waves with a frequency of 200 Hz were induced parallel to the B_0-field direction (z) by a copper coil fixed to a pivoting carbon fiber rod connected with the surface of the gel. The excitation device was fixed to the standard head coil of a clinical scanner (1.5 T, Siemens, Erlangen, Germany). Data were acquired using a modified gradient echo technique, FLASH (*F*ast *L*ow *A*ngle *Sh*ot, $T_R/T_E = 40/12$ ms, field of view 160 mm, matrix 256 × 256 pixel, 12 s acquisition time), sensitized to particle displacement by sinusoidal wave-encoding gradients. Motion-sensitive phase images were used for the analysis.

Representative experimental results are displayed in the first row of Figure 1. Several regions may be differentiated: (a) the solidified part (peripheral regions) with well-delineated wave patterns, (b) the transition zone, where smaller wavelengths suggest decreased stiffness, and (c) the fluid region, where no waves can be detected. Occasionally, reflected waves can be seen at the boundaries of the different compartments. With increasing time, the fluid part shrinks and the transition zone broadens until final solidification.

In a first approach wave patterns and correlating elastograms were reproduced using a model of externally driven coupled harmonic oscillators (CHO).[5] Adjacent volume elements were coupled horizontally and vertically by 2D arrays of coupling constants $k(x,y,t)$. The elements of $k(x,y,t)$ were expressed in terms of wave propagation speeds equal to the square root of the shear stiffness of agar. The experimental data indicate that $k(x,y,t)$ varies from a maximum coupling (c_{max}) in the peripheral solidified parts to low values in the fluid parts. With decreasing temperature gradients the transition zone enlarges, the slope flattens, and $k(x,y,t)$ increases to c_{max} in the central parts. As scan time is short compared to cooling time, the time dependence of $k(x,y,t)$ may be separated. Using a coupling profile $\mathcal{R}(x,y)$ that is fitted to an observed shear stiffness (at $t = t_M$) $k(x,y,t)$ then evolves in time according to

$$k(x,y,t) = c_{max} \cdot \mathcal{R}(x,y)^{f(t)}; \quad 0 < \mathcal{R}(x,y) < 1$$

with

$$f(t) > 1 \text{ for } 0 < t < t_M, \quad f(t) = 1 \text{ for } t_M = 0, \quad \text{and } f(t) < 1 \text{ for } t > t_M$$

To fit a complete series of time-resolved MRE wave images the following parameters had to be varied: (i) maximum coupling (i.e., wave propagation speed) c_{max}, (ii) $f(t)$ with t_M, and (iii) the form the 2D contour function $\mathcal{R}(x,y)$. Best fits to experimental data were found by supervised iteration for an inverse 2-dimensional Gaussian profile $\mathcal{R}(x,y)$ and an exponential $f(t)$ according to

$$\mathcal{R}(x,y) = 1 - a_1 \exp[-(x-x_0)^2/\sigma_x^2 - (y-y_0)^2/\sigma_y^2]$$

$$f(t) = a_2^{-(t-t_M)/\Delta t}; \quad a_2 > 1$$

with a time step size $\Delta t = 3.0$ min between each simulated wave image, $t_M = 243$ min, off-center positions x_0 and y_0 at two-thirds of object size, halfwidths of 73% (σ_x) and 67% (σ_y) of object size, and constant factors $a_1 = 0.9$ and $a_2 = 1.1$. c_{max} was found to be 2.9 m/s. c_{max} and Δt could be varied by ±0.2 m/s respective ±0.5 min without effective changes in the calculated wave patterns. From c_{max} a shear stiffness of 5.9 ± 0.2 kN/m^2 was determined. The results of the simulated wave patterns and the corresponding coupling matrixes are displayed in Figure 1.

To reproduce the experimental conditions, the transverse excitation of the coupled oscillators occurred at the position of the shear wave excitation plate. An additional small excitation with amplitudes of one-fifth of the initial shear waves was applied

* To whom correspondence should be addressed. Telephone: +49-30-8445-4506. Fax: +49-30-8445-4510. E-mail braun@medizin.fu-berlin.de.
† Free University Berlin.

(1) (a) Muthupillai, R.; Lomas, D. J.; Rossman, P. J.; Greenleaf, J. F.; Manduca, A.; Ehman, R. L. *Science* **1995**, *269*, 1854−1857. (b) Bishop, J.; Poole, G.; Leitch, M.; Plewes, D. B. *J. Magn. Reson. Imaging* **1998**, *8*, 1257−1265. (c) Chenevert, T. L.; Skovoroda, A. R.; O'Donnell, M.; Emelianov, S. Y. *Magn. Reson. Med.* **1998**, *39*, 482−490.

(2) (a) Kruse, S. A.; Smith, J. A.; Lawrence, A. J.; Dresner, M. A.; Manduca, A.; Greenleaf, J. F.; Ehman, R. L. *Phys. Med. Biol.* **2000**, *45*, 1579−1590. (b) Plewes, D. B.; Bishop, J.; Samani, A.; Sciarretta, J. *Phys. Med. Biol.* **2000**, *45*, 1591−1610. (c) Sinkus, R.; Lorenzen, J.; Schrader, D.; Lorenzen, M.; Dargatz, M.; Holz, D. *Phys. Med. Biol.* **2000**, *45*, 1649−1664.

(3) Sarvazyan, A. P.; Skovoroda, A. R.; Emelianov, S. Y.; Fowlkes, J. B.; Pipe, J. G.; Adler, R. S.; Buxton, R. B.; Carson, P. L. In *Acoustical Imaging*; Jones, J. P., Ed.; New York: Plenum Press, 1995; Vol. 21.

(4) (a) Manduca, A.; Oliphant, T. E.; Dresner, M. A.; Mahowald, J. L.; Kruse, S. A.; Amromin, E.; Felmlee, J. P.; Greenleaf, J. F.; Ehman, R. L. *Med. Image Anal.* **2001**, in press. (b) Bishop, J.; Samani, A.; Sciarretta, J.; Plewes, D. *Phys. Med. Biol.* **2000**, *45*, 2081−2091. (c) Oliphant, T. E.; Manduca, A.; Ehman, R. L.; Greenleaf, J. F. *Magn. Reson. Med.* **2001**, *45*, 299−310. (d) Van Houten, E. E.; Paulsen, K. D.; Miga, M. I.; Kennedy, F. E.; Weaver, J. B. *Magn. Reson. Med.* **1999**, *42*, 779−786.

(5) (a) Sack, I.; Buntkowsky, G.; Bernarding, J.; Tolxdorff, T.; Braun J.; *Proc. SPIE* **2001**, *4320*, 868−874. (b) Braun, J.; Buntkowsky, G.; Bernarding, J.; Tolxdorff, T.; Sack, I. *Magn. Reson. Imaging* **2001**, *19*, 703−713.

10.1021/ja016141y CCC: $20.00
Published on Web 10/13/2001

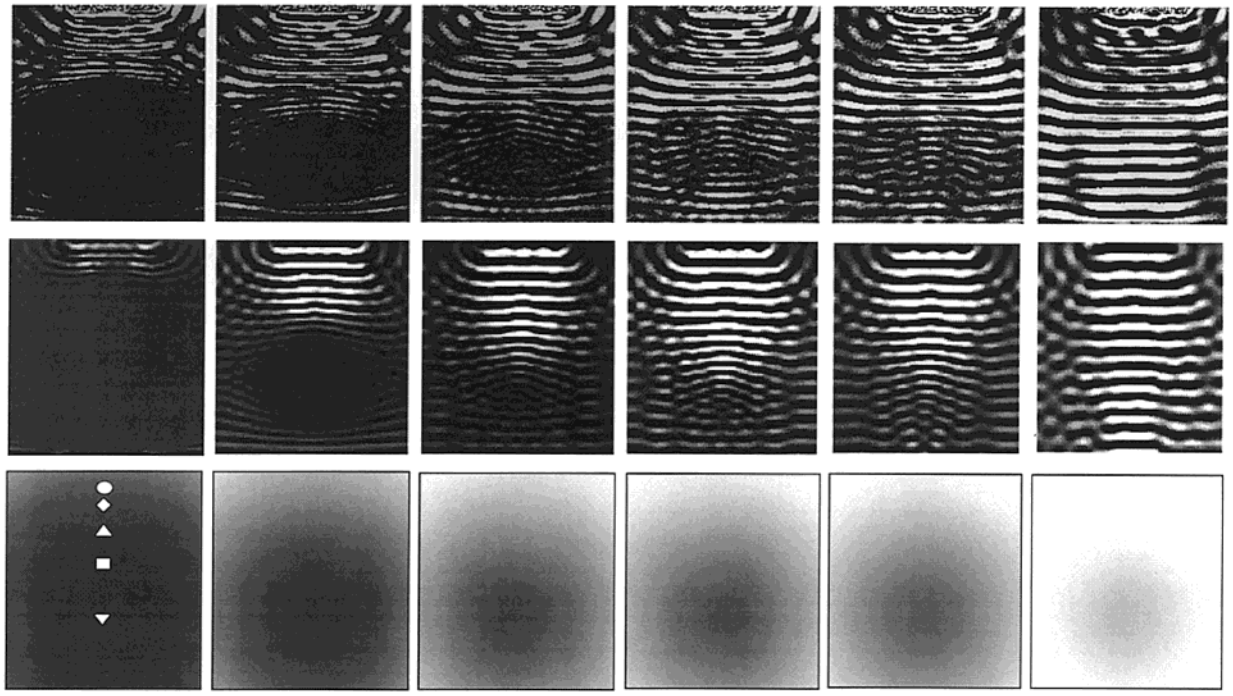

Figure 1. MRE images showing the solidification of an agar gel. Upper row: experimental MRE images (time [min]: 205, 236, 256, 261, 267, 300). The temperature decreases from left to right. Observed wavenumbers depend on the local elasticity of the gel. Low wavenumbers represent a higher speed of wave propagation and therefore a stiffer environment compared to regions characterized by lower wave speed. The absence of waves indicates the fluid sol state. Middle row: CHO calculations for the simulation of the observed temperature-dependent wave patterns. Lower row: input coupling matrixes for the simulations. The discrepancy between experiment and simulation at the highest temperature (left image) may be due to a local shift of the transition zone of the coupling contour function.

to the bottom of the object to simulate vibrations induced by the scanner. The local attenuation of the waves was adjusted within the object equivalent to the square of the shear stiffness profile, that is, $\mathcal{R}^2$, and at the edges with the strongest possible damping to avoid reflections.[5] Figure 2 displays the time evolution of the simulated shear stiffness of selected positions during gelation.

The measurement of viscoelastic properties is a powerful tool in the characterization of gel networks.[6] In many cases, viscoelastic properties are much more sensitive to relatively small changes in the network structure than other, independent techniques, for example, small-angle X-ray scattering, small-angle neutron scattering, optical rotation, infrared spectroscopy, and nuclear magnetic resonance spectroscopy.[7] As demonstrated by the results, MRE has the advantage of a spatially high-resolved characterization of elastic properties. The local shear stiffness can subsequently be determined by applying the approach based on CHO calculations.

Assuming a time-dependent exponentially scaled Gaussian stiffness contour function allowed a description of the dynamics of the gelation process. A good correlation with the experimental data could be observed in the case of moderate temperature gradients in the sample and an extensive organization of the intermolecular network. The value of 5.9 ± 0.2 kN/m^2 for the shear stiffness of agar (1.5%) at room temperature is in good agreement with the literature.[8]

The spatial resolution of MRE for the detection of sudden changes in elastic properties is limited by the minimum pixel size provided by the gradient system.

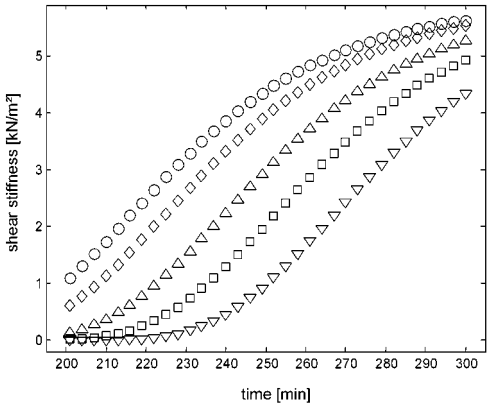

Figure 2. Calculated shear stiffness as a function of time and location. Locations are indicated by ○ ◇ △ □ ▽, respectively, in Figure 1. For further explanations see text.

While in our case the minimum pixel size was on the order of 0.2 mm, other gradient systems used for micro-imaging may allow a higher spatial resolution down to several tens of micrometers. The mechanical excitation frequency was limited by the rise time of the gradient system to about 1 kHz. Nevertheless, combining the advantages of a noninvasive and nondestructive technique with the simultaneous, spatially resolved determination of elasticity properties over an entire sample using rheological and other mentioned techniques should help to gain a deeper insight into the spatially resolved dynamics of the cross-linking process of thermo-reversible gels. For further quantitative investigations, MR-based temperature measurements should be included to obtain $k(x,y,t)$ from thermodynamical properties of the sample.

JA016141Y

(6) (a) Nishinari, K. *J. Appl. Phys.* **1976**, *15*, 1263−1269. (b) Clark, A. H.; Richardson, R. K.; Ross-Murphy, S. B.; Stubbs, J. M. *Macromolecules* **1983,** *16*, 1367−1370. (c) Watase, M.; Nishinari, K. *Rheol. Acta* **1983**, *22*, 580−584. (d) Watase, M.; Nishinari, K. *Polym. J.* **1986**, *18*, 1017−1020. (e) Guiseley, K. B. *Carbohydr. Res.* **1970**, *13*, 247−253.

(7) te Nijenhuis, K. *Adv. Polym. Sci.* **1997**, *130*, 1−252.

(8) Watase M.; Nishinari, K.; Clark, A. H.; Ross-Murphy, S. B. *Macromolecules* **1989**, *22*, 1196−1201.